

All-optical fiber anemometer based on laser heated fiber Bragg gratings

Shaorui Gao,¹ A. Ping Zhang,^{1,*} Hwa-Yaw Tam,² L. H. Cho,² and Chao Lu²

¹*Center for Optical and Electromagnetic Research, State Key Laboratory of Modern Optical Instrumentation, Zhejiang University, Hangzhou 310058, China*

²*Photonics Research Center, The Hong Kong Polytechnic University, Kowloon, Hong Kong SAR, China*

*zhangap@zju.edu.cn

Abstract: A fiber-optic anemometer based on fiber Bragg gratings (FBGs) is presented. A short section of cobalt-doped fiber was utilized to make a fiber-based “hot wire” for wind speed measurement. Fiber Bragg gratings (FBGs) were fabricated in the cobalt-doped fiber using 193 nm laser pulses to serve as localized temperature sensors. A miniature all-optical fiber anemometer is constructed by using two FBGs to determine the dynamic thermal equilibrium between the laser heating and air flow cooling through monitoring the FBGs’ central wavelengths. It was demonstrated that the sensitivity of the sensor can be adjusted through the power of pump laser or the coating on the FBG. Experimental results reveal that the proposed FBG-based anemometer exhibits very good performance for wind speed measurement. The resolution of the FBG-based anemometer is about 0.012 m/s for wind speed range between 2.0 m/s and 8.0 m/s.

©2011 Optical Society of America

OCIS codes: (060.2370) Fiber optics sensors; (060.3735) Fiber Bragg gratings; (060.2340) Fiber optics components.

References and links

1. B. Lee, “Review of the present status of optical fiber sensors,” *Opt. Fiber Technol.* **9**(2), 57–79 (2003).
2. A. D. Kersey, M. A. Davis, H. J. Patrick, M. LeBlanc, K. P. Koo, C. G. Askins, M. A. Putnam, and E. J. Friebele, “Fiber grating sensors,” *J. Lightwave Technol.* **15**(8), 1442–1463 (1997).
3. I. Bennion, and L. Zhang, “Fiber Bragg grating technologies and applications in sensors,” *2006 OSA/OFC*, 2415–2417 (2006).
4. B. O. Guan, H. Y. Tam, S. L. Ho, W. H. Chung, and X. Y. Dong, “Simultaneous strain and temperature measurement using a single fibre Bragg grating,” *Electron. Lett.* **36**(12), 1018–1019 (2000).
5. G. H. Chen, L. Y. Liu, H. Z. Jia, J. M. Yu, L. Xu, and W. C. Wang, “Simultaneous strain and temperature measurements with fiber Bragg grating written in novel Hi-Bi optical fiber,” *IEEE Photon. Technol. Lett.* **16**(1), 221–223 (2004).
6. J. F. Ding, A. P. Zhang, L. Y. Shao, J. H. Yan, and S. He, “Fiber-taper seeded long-period grating pair as a highly sensitive refractive-index sensor,” *IEEE Photon. Technol. Lett.* **17**(6), 1247–1249 (2005).
7. A. P. Zhang, L. Y. Shao, J. F. Ding, and S. He, “Sandwiched long-period gratings for simultaneous measurement of refractive index and temperature,” *IEEE Photon. Technol. Lett.* **17**(11), 2397–2399 (2005).
8. M. Stieglmeier and C. Tropea, “Mobile fiber-optic laser Doppler anemometer,” *Appl. Opt.* **31**(21), 4096–4105 (1992).
9. G. D. Byrne, S. W. James, and R. P. Tatam, “A Bragg grating based fibre optic reference beam laser Doppler anemometer,” *Meas. Sci. Technol.* **12**(7), 909–913 (2001).
10. S. Takashima, H. Asanuma, and H. Niitsuma, “A water flowmeter using dual fiber Bragg grating sensors and cross-correlation technique,” *Sens. Actuators A Phys.* **116**(1), 66–74 (2004).
11. O. Frazão, P. Caldas, F. M. Araújo, L. A. Ferreira, and J. L. Santos, “Optical flowmeter using a modal interferometer based on a single nonadiabatic fiber taper,” *Opt. Lett.* **32**(14), 1974–1976 (2007).
12. H. H. Bruun, *Hot-Wire Anemometry: Principles and Signal Analysis* (Oxford University Press, 1995).
13. K. P. Chen, L. J. Cashdollar, and W. Xu, “Controlling fiber Bragg grating spectra with in-fiber diode laser light,” *IEEE Photon. Technol. Lett.* **16**(8), 1897–1899 (2004).
14. R. Slavík and M. Kulishov, “Active control of long-period fiber-grating-based filters made in erbium-doped optical fibers,” *Opt. Lett.* **32**(7), 757–759 (2007).
15. K. P. Chen, B. McMillen, M. Buric, C. Jewart, and W. Xu, “Self-heated fiber Bragg grating sensors,” *Appl. Phys. Lett.* **86**(14), 143502 (2005).
16. B. McMillen, C. Jewart, M. Buric, K. P. Chen, Y. Lin, and W. Xu, “Fiber Bragg grating vacuum sensors,” *Appl. Phys. Lett.* **87**(23), 234101 (2005).

17. M. Buric, K. P. Chen, M. Bhattacharai, P. R. Swinehart, and M. Maklad, "Active fiber Bragg grating hydrogen sensors for all-temperature operation," *IEEE Photon. Technol. Lett.* **19**(5), 255–257 (2007).
18. D. W. Lamb and A. Hooper, "Laser-optical fiber Bragg grating anemometer for measuring gas flows: application to measuring the electric wind," *Opt. Lett.* **31**(8), 1035–1037 (2006).
19. C. Jewart, B. McMillen, S. K. Cho, and K. P. Chen, "X-probe flow sensor using self-powered active fiber Bragg gratings," *Sens. Actuators A Phys.* **127**(1), 63–68 (2006).
20. S. Takagi, "A hot-wire anemometer compensated for ambient temperature variations," *J. Phys. E Sci. Instrum.* **19**(9), 739–743 (1986).

1. Introduction

With the development of photosensitivity and grating fabrication technologies, optical fiber gratings have become an important enabling technology for the realization of many optical sensors for a wide variety of measurements [1–7]. Due to their many advantages, e.g. compactness, high sensitivity, fast response, electromagnetic immunity and multiplexing capability, a variety of sensors such as strain and temperature sensors [4,5], refractive index sensors [6,7], have been developed by using fiber Bragg gratings (FBGs) or long-period gratings (LPGs). In recent years, researchers are continuously making efforts to develop fiber grating sensors to measure different parameters for various industrial applications. This permits the use of a single interrogator to deal with many FBGs to measure various kinds of parameters and could eventually increase the cost effectiveness of FBG sensor systems.

One kind of FBG-based sensor being developed is optical fiber anemometer or flowmeter for the measurement of gas or liquid flow speed. FBG-based anemometer can find widespread applications, for example in wind turbines where FBG sensors are being actively investigated to measure temperature, strain and vibration of wind turbine blades. Although many kinds of anemometers and flow-meters have been developed using different principles [8–11], e.g. laser Doppler technology [8,9], cross-correlation technique [10] or fiber modal interferometer [11], the classical hot-wire anemometry is still an irreplaceable approach for wind speed measurement particularly for the investigations of rapidly varying flows and turbulences [12].

Hot-wire anemometry (HWA) is based on the heat transfer from sensors to the surrounding environment. In order to achieve a localized hot fiber section, one can use attenuation or active fibers [13,14] for making spectrum controllable FBGs or LPGs. Compared with passive fiber grating sensors, laser controlled fiber grating sensors have some enhanced features like controllable sensitivity, responsivity, and dynamic range to enable measurement in large temperature range [15–17]. D. W. Lamb et al. proposed a low-cost FBG anemometer externally heated by using a CO₂ laser for measuring gas flow in the high-voltage environment (corona discharge) [18]. However, such sensor may be too bulky for some industrial applications. Thereafter, C. Jewart et al. proposed a flowmeter based on two cross-mounted thin-silver coated FBGs internally heated by laser light for measuring the magnitude and direction of gas flow [19].

In this paper, we proposed an FBG-based anemometer where a laser beam is used to heat

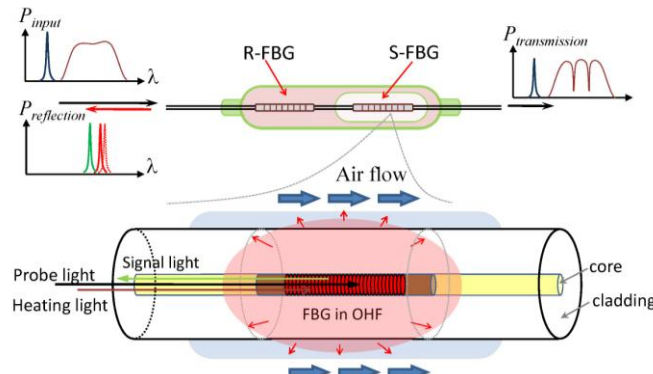


Fig. 1. Schematic diagram and work principle of the all-optical fiber anemometer based on laser-heated fiber Bragg gratings.

the FBG directly, and the rate of heat loss from the FBG is measured from its wavelength shift. The FBG was inscribed in a fiber that was co-doped with light absorption materials such as cobalt or neodymium. Figure 1 show two FBGs (S-FBG and R-FBG) written in the light absorption fiber that serve as sensing and reference elements, respectively. The pump laser is launched into the fiber core and the temperature of the FBGs rises through nonradiative absorption. Broadband light at different wavelength band is used as the probe light to monitor the Bragg wavelength of the laser-heated FBGs (LHFBGs). One can measure the air flow induced heat transfer through monitoring the Bragg wavelengths of the S-FBG. The R-FBG is packaged with heat-insulation tube for monitoring the laser power variation. Experimental results show that the proposed FBG-based anemometer performs very well in measuring wind speed.

2. Fabrication of the LHFBGs

Fiber Bragg gratings inscribed in two light absorption fibers fabricated by CorActive High-Tech, Inc., with different absorption coefficients, were used in the wind speed measurement experiment. The S-FBG was inscribed in the fiber with a higher light absorption coefficient and thus could be heated to a higher temperature to achieve large dynamic range of measurement. The absorption coefficient of the fiber used for the fabrication of the S-FBG is 5 dB/cm at 1480 nm pump wavelength. The other fiber with absorption coefficient of 1 dB/cm at 1480 nm was used for the fabrication of the R-FBG. All FBGs were fabricated with a 193-nm ArF excimer laser (Coherent, Bragg Star S-Industrial) using the phase mask technique. The period of the phase mask is 1070 nm.

Figure 2 shows the measured transmission and reflection spectra of the S-FBG and R-FBG and the temperature dependences of their central wavelengths. The length of the two gratings is ~5 mm and written in 7-mm long of the light absorption fibers. The central wavelength and the transmission dip of the S-FBG are 1546.31 nm and -5.33 dB, respectively, while the central wavelength and the transmission dip of the R-FBG are 1544.54 nm and -5.07 dB, respectively. Both the probe and pump lights were launched from the R-FBG side and therefore light reflected from the R-FBG is slightly stronger than that from the S-FBG. The temperature sensitivity of the R-FBG and S-FBG are 12.2 and 11.8 pm/°C, respectively.

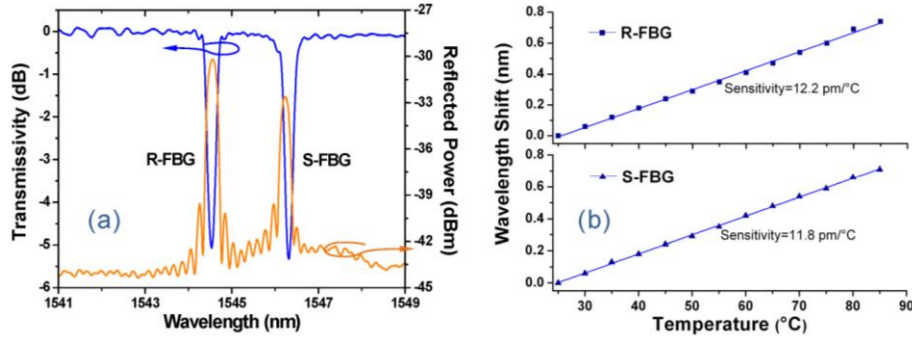


Fig. 2. Transmission and reflection spectra of the R-FBG and S-FBG (a) and the temperature dependences of the central wavelengths of the two FBGs (b).

Figure 2(b) shows the wavelength shift of the FBGs with respect to temperature. In practical applications, one has to take into account the temperature cross-sensitivity of the sensor in measuring wind speed. In general, the variation of air temperature is quite slow and therefore one could switch off the pump laser and allows the S-FBG to cool down before using it to measure the air temperature. Alternatively, one could use another FBG fabricated in the standard SMF and connected to the S-FBG for temperature measurements, which is a common approach used in HWA [20].

Figure 3 shows the spectra of the two LHFBGs heated by light from a 1480 nm semiconductor laser. Figure 3(a) presents the dependence of the reflection spectra of the two

LHFBGs on the power of the pump laser. Both reflection peaks of the two FBGs shift to longer wavelength with increasing pumping power. The S-FBG exhibits a larger wavelength shift because of its higher absorption coefficient and therefore was heated more efficiently than the R-FBG. Figure 3(b) shows the dependence of the central wavelength of the two LHFBGs on pump power. When the power of pump laser increases from 0 mW to 305 mW, the central wavelength of S-FBG linearly shifts from 1546.24 nm to 1548.46 nm, while the central wavelength of R-FBG only shifts from 1544.56 nm to 1545.21 nm. If we assume the total loss of the two fusion splices and the 7-mm long low light-absorption fiber is about 1 dB, then the optical power of the pump light reaches S-FBG is about 80% of that reaches the R-FBG. One can thus deduce that the pumping power consumed in the S-FBG is more than 3 times of that consumed in the R-FBG.

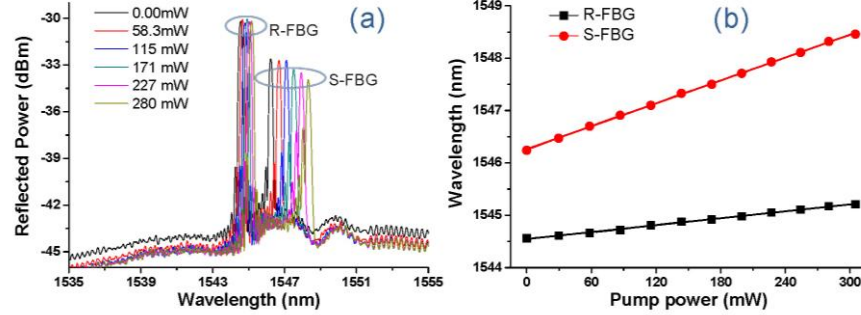


Fig. 3. Reflection spectra (a) and central wavelengths (b) of the LHFBGs with increasing power of the 1480 nm pump laser.

3. LHFBG based anemometer

The two LHFBGs formed an all-optical fiber anemometer. In order to reduce heat transfer, the R-FBG was sealed inside a thin alundum tube with an inner diameter of 0.6 mm and outer diameter of 2-mm. The packaged R-FBG and the unpackaged S-FBG were installed inside a specially designed stainless steel tube which has an inner diameter and outer diameter of 3 mm and 4 mm, respectively. Convection slots were made in the stainless steel tube to allow S-FBG to expose to open air. Epoxy adhesive was used to bond the fiber inside the tubes.

Figure 4 shows the experimental setup for testing of the FBG-based anemometer. A commercial wind tunnel (SANLING KQD-03, Scientific & teaching instruments factory of ECNU) and an electrical HWA (DANTEC, Stream Line 90N10 Frame) were used to evaluate the performance of the FBG-based anemometer. The wind speed of the wind tunnel can be varied from 0 to 8.0 m/s. The dimension of the wind tunnel outlet is 25.4 cm by 25.4 cm. The FBG-based anemometer and the electrical anemometer were fixed around the outlet so that same wind speed passed around the two anemometers. The 1480 nm laser light is launched to the FGB-based anemometer through a 1480/1550 wavelength-division multiplexer (WDM). The probe light emitted from the FBG interrogator is also launched to the fiber through an optical circulator and the WDM, to interrogate the LHFBGs. The resolution and sampling frequency of the FBG interrogator are 1.0 pm and 25 Hz, respectively.

HWA is based on the heat-transfer principle and thus the sensitivity of the sensor depends

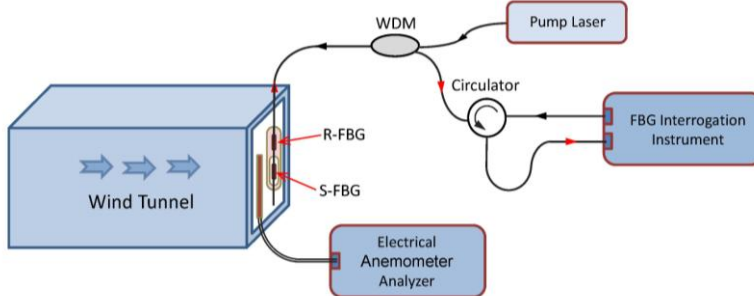


Fig. 4. The schematic diagram of the setup for test of the LHFBG anemometer.

on the heat transfer rate from the sensor to the surrounding environment. One of the two LHFBG anemometers was recoated with epoxy to evaluate the coating's effects on the sensor performance. The diameter of the recoated fiber anemometer is ~ 0.5 mm. In order to evaluate the effects of pumping power on the sensor performance, the LHFBGs were pumped at three different powers with the 1480 nm laser.

In the experiments, the wind speed in the wind tunnel is manually adjusted. The wind speed and the central wavelengths of the LHFBGs were recorded by using the electrical anemometer and the FBG interrogator, respectively. The minimum wind speed that can be set by the wind tunnel is around 1.5 m/s. Figure 5 shows the measured sensor responses to different wind speeds. When the power of pump laser is 84.05 mW and no wind flow, the central wavelengths of the R-FBG and the S-FBG are 1543.803 nm and 1546.747 nm, respectively. When the wind speed is increased from 0 to 8 m/s, the central wavelength of the S-FBG shifts to shorter wavelength, while the central wavelength of the R-FBG is almost unchanged. The sensitivity of the LHFBG anemometer is quite high when the wind speed is low, and becomes lower at high wind speed. The sensitivity degradation is similar to that experienced by electrical anemometers as more heat is dissipated at higher wind-speed. When the power of the pump laser is increased from 84 mW to 299.3 mW, the anemometer exhibits similar behavior but reveals higher sensitivity. Therefore, a simple solution to improve the sensitivity of the LHFBG anemometer at high wind-speed conditions is to increase the pump power.

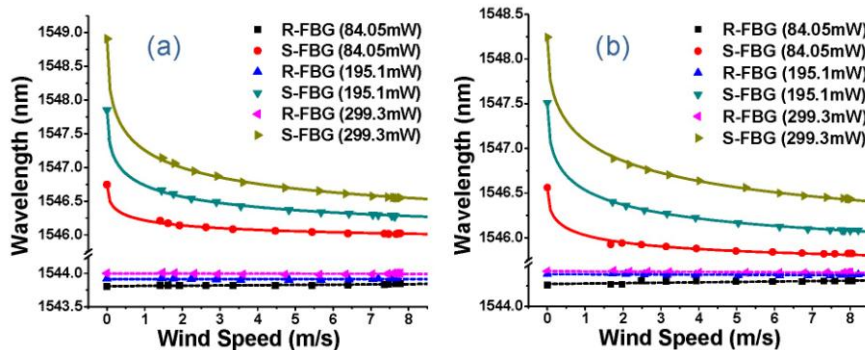


Fig. 5. Measured central wavelengths versus wind speed of the FBG-based anemometer under different pumping powers. The solid curves are fitted by using the derived equation. (a) S-FBG without coating; (b) Recoated S-FBG.

Based on the theory of hot-wire anemometer [12], one can write the relationship between the heat loss, H_{loss} , and the wind speed, v , as:

$$H_{loss} = [T_a(v) - T_e] \left(A + B\sqrt{v} \right), \quad (1)$$

where T_a is the temperature of the anemometer, T_e is the temperature of the environment, A and B are empirical calibration constant. Based on the rule of energy conservation, the heat loss should equal to the power consumption of the S-FBG, i.e.

$$H_{loss} = P_{input}(1 - a_r)a_s, \quad (2)$$

where P_{input} is the input laser power, a_r is the absorption coefficient of the R-FBG, and a_s is the absorption coefficient of the S-FBG.

Moreover, the dependence of the wavelength shift of FBG, $\Delta\lambda$, on the change of temperature, $\Delta T = T_a(v) - T_a(0)$, is well known as

$$\Delta\lambda / \lambda_{h0} = (\alpha + \xi)\Delta T, \quad (3)$$

where λ_{h0} is the wavelength of heated FBG before wind blowing, and α is the thermal expansion coefficient, and ξ is the thermo-optic coefficient. Using Eqs. (1) and (3), one can thus deduce the dependence of the wavelength shift of the LHFBG anemometer on the wind speed as,

$$\Delta\lambda = \lambda_{h0}(\alpha + \xi)[H_{loss} / (A + B\sqrt{v}) - \Delta T_0], \quad (4)$$

where $\Delta T_0 = T_a(0) - T_e$. If one writes the wavelength of the FBG before heating as λ_{e0} , the above equation can be further written as

$$\lambda(v) - \lambda_{e0} = \lambda_{h0}(\alpha + \xi)H_{loss} / (A + B\sqrt{v}), \quad (5)$$

The solid curves in Fig. 5 show the fitted results using the above equation. One can see that the experimental results agreed very well with the theory of hot-wire anemometer.

Since the anemometers have non-linear responses in the range of wind speed between 2.0 m/s and 8.0 m/s, as shown in Fig. 5, we use the slopes of linearly fitted data as the effective sensitivity in this specific range to evaluate the effects of the pump power and the recoating on the sensor performance. Figure 6 presents the calculated effective sensitivities of the two anemometers with and without coating. One can see that the sensitivities of the two anemometers increase with pumping power. The recoating process can reduce the sensitivity of the anemometer. Based on the calculated sensitivity and the resolution of the FBG interrogator, i.e. 1 pm, one can thus deduce that the resolution of wind speed measurement with the anemometer is ~ 0.012 m/s for wind speed ranges from 2 m/s to 8 m/s.

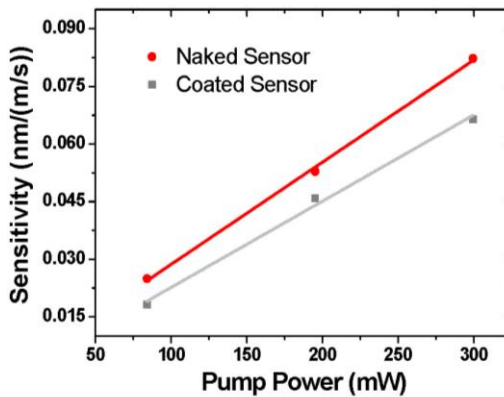


Fig. 6. Effective sensitivities of the recoated and naked anemometers at different pump powers.

The dynamic response of the LHFBG anemometer was also evaluated experimentally. The anemometer was installed behind a shutter and abruptly blown by air when the shutter is opened. Figure 7(a) and 7(b) present two groups of measured dynamic responses of the anemometer pumped at different power levels. One can see that the dynamic response of this anemometer depends significantly on the wind speed. The response time decreases from 700 ms to 200 ms when the wind speed rises from 1.0 m/s to 4.5 m/s. By comparison, the dynamic response is not very sensitive to the pump-power level. Figure 7(c) shows the response time is relatively independent of the pump power when it was increased from 98 mW to 218 mW.

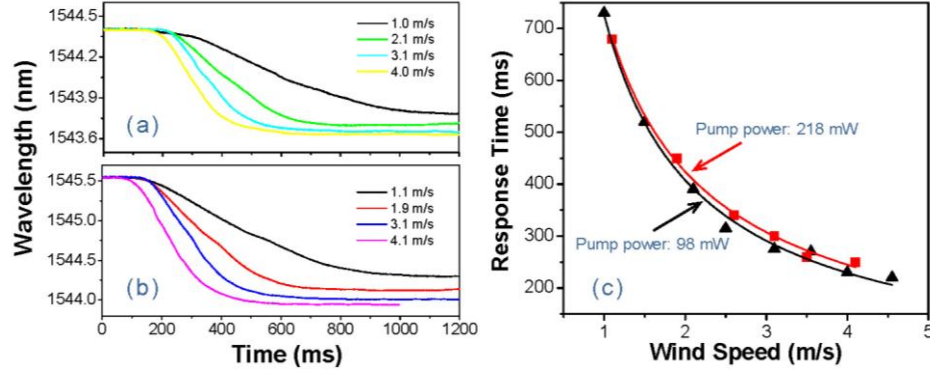


Fig. 7. Dynamic responses of the LHFBG anemometer pumped at different power levels: (a) pump power is 98 mW; (b) pump power is 218 mW; (c) response time versus wind speed.

4. Conclusion

We have presented the fabrication and test results of LHFBG based anemometers using FBGs inscribed in light-absorption fibers. Experimental results show that the cobalt-doped fiber can absorb light efficiently to heat an FBG to become a “hot-wire” without metal coating. The fabricated LHFBG anemometers have been tested inside a commercial wind tunnel and calibrated using a commercial electrical anemometer. The findings show that the performance of the FBG-based anemometer can be predicted accurately using the theory of conventional hot-wire anemometry. The effects of pump powers and recoating on the sensor sensitivities have been investigated for wind speed ranged from 2 m/s to 8 m/s. Coupled with the many advantages of optical fiber sensors such as electromagnetic immunity, multiplexing and remote sensing capability, the proposed single-fiber LHFBG anemometer holds great potential for many industrial applications.

Acknowledgments

The authors thank Prof. Xueming Shao, Department of Mechanics of Zhejiang University, for the support of wind speed measurement. This work was supported by the Fundamental Research Funds for the Central Universities.